Proceedings of the 11th ICPMG 2026
11th International Conference on Physical Modelling in Geotechnics
8-12 June 2026, Zurich, Switzerland

Study on liquefaction countermeasure for existing road bridge pile foundations in volcanic ash ground

T. Egawa, M. Yamaki
Civil Engineering Research Institute for Cold Region, Sapporo, Japan, egawa@ceri.go.jp, yamaki-m@ceri.go.jp

K. Isobe
Hokkaido University, Sapporo, Japan, kisobe@eng.hokudai.ac.jp

ABSTRACT: This study used centrifuge model tests to examine the applicability of a seismic reinforcement method that is to be used when pile foundation stability is compromised solely due to the liquefaction of volcanic ash ground. The method involves enclosing the ground around the pile foundation using grid-form ground improvement walls that are installed without making contact with the existing pile foundation. In the tests, three types of pile foundations that were widely used in Hokkaido before the introduction of current seismic design standards were selected to evaluate how the distance between the piles and walls and the strength of the improved ground affect the liquefaction resistance of the foundation and the behavior of the piles. It was found that a maximum grid spacing of 7.0 meters and a minimum clearance of 2.0 meters from the center of the outermost pile to the wall effectively suppress the reduction in the coefficient of horizontal subgrade reaction of pile, while avoiding adverse effects on the overall seismic design of the bridge.

1 INTRODUCTION

In Japan, seismic countermeasures for existing road bridges are being promoted to reduce the risk of major earthquakes that are expected to occur. Some pile foundations of road bridges that were constructed before the current earthquake resistance standards were established do not satisfy the design standards. While there are pile foundations that require increased proof stress, there are also pile foundations that are able to satisfy the current seismic design standards even just through the control of liquefaction of the surrounding ground. This situation is also true for pile foundations in the volcanic ash coarse-grained soils that are widely distributed in Hokkaido and Kyushu and are treated as problem soils in Japan.

Based on the above, we have been investigating the applicability of a ground improvement technique that uses grid-form walls, in which the ground around the pile foundation is enclosed by improvement walls that are not in contact with the existing structure. Grid-form ground improvement walls were devised as a seismic reinforcement technique that is applicable in cases where the stability of the pile foundation is compromised only by the liquefaction of volcanic ash ground. As an aseismic reinforcement technique for pile foundations constructed in a liquefiable volcanic ash ground, we experimented on ground improvement walls that enclose a pile foundation without coming in contact with it. The effectiveness of this aseismic reinforcement technique in controlling the shear deformation and liquefaction of the ground inside the walls was investigated.

This study focuses on steel pipe piles (SPP) with a diameter of 500 mm, in-situ cast concrete piles (CCP) with a diameter of 1,000 mm, and precast concrete piles (PCP) with a diameter of 300 mm. Centrifugal model tests and dynamic effective stress analysis were used to evaluate the effectiveness of a ground improvement method for grid-form walls at suppressing liquefaction and its impact on existing piles.

This study examines the optimal spacing of grid-form ground improvement walls, the optimal distance from the outermost pile center, and the improvement strength required for retrofitting road bridge pile foundations built before the current seismic standards. These findings were derived by integrating new experimental results for PCP with existing centrifugal model tests of SPP and CCP (Egawa et al., 2024).

2 OUTLINE OF THE CENTRIFUGAL MODEL TESTS

The centrifugal model tests utilized a centrifugal beam loading apparatus with a radius of 2.5 m owned

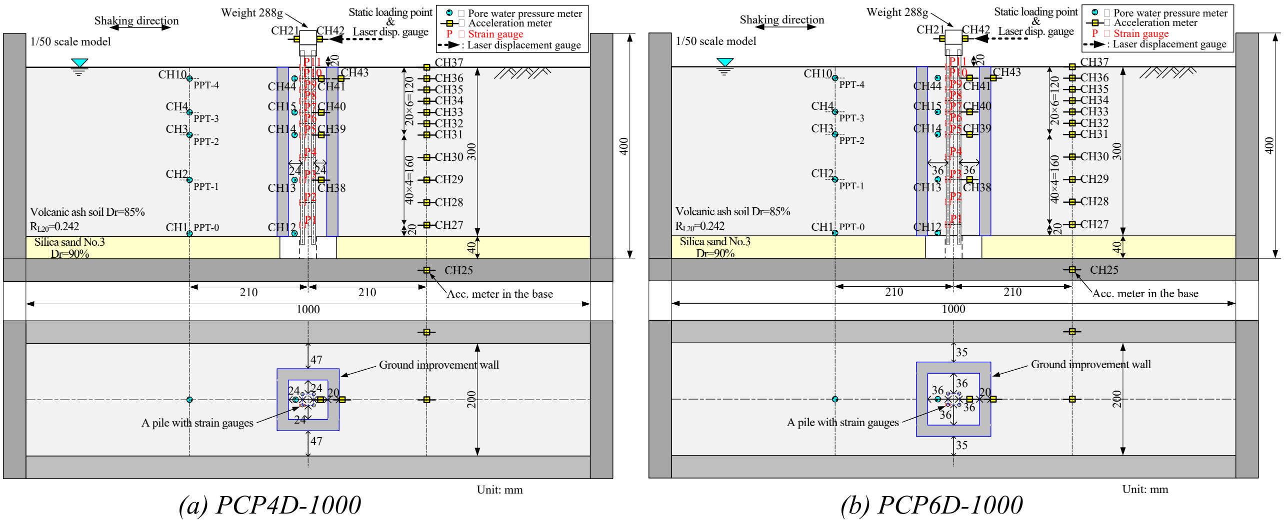

(a) PCP4D-1000 (b) PCP6D-1000

Figure 1. Overview of the experimental models for PCP.

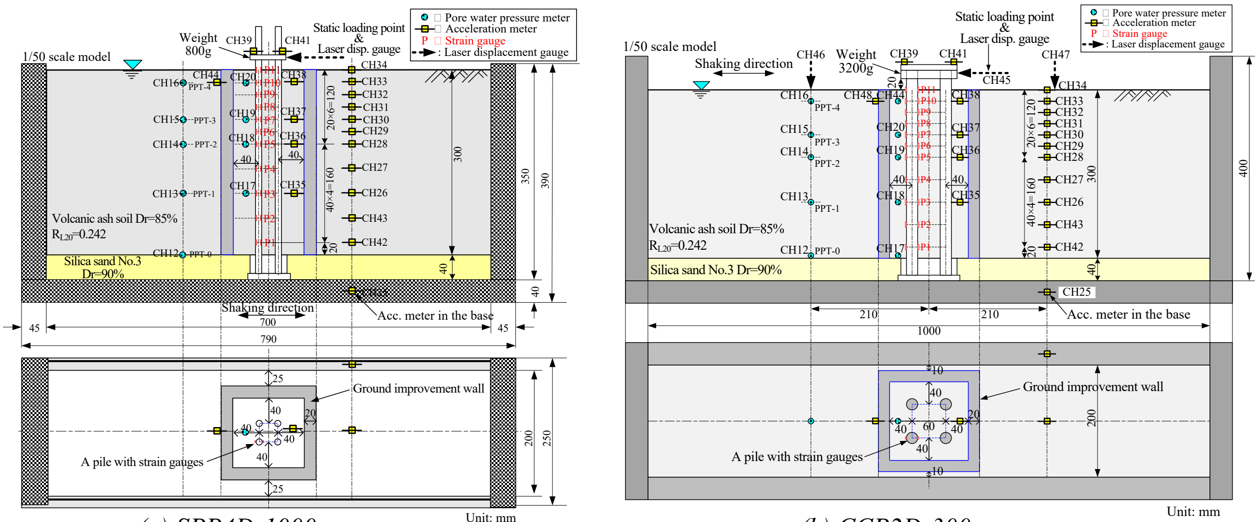

(a) SPP4D-1000 (b) CCP2D-300

Figure 2. Overview of experimental models for SPP and CCP. (Egawa et al., 2024)

by the Civil Engineering Research Institute for Cold Region. Table 1 shows test cases for PCP. Figure 1 shows schematics of experimental models PCP4*D*-1000 and PCP6*D*-1000. Additionally, Figure 2 shows overviews of experimental models SPP4*D*-1000 and CCP2*D*-300 from Egawa et al. (2024) for reference. A rigid soil tank was employed, but the target evaluation area was located at a sufficient distance from the side walls to minimize boundary effects, including reflected shear waves.

The centrifugal model tests consisted of static horizontal loading tests followed by dynamic excitation tests. In both tests, a centrifugal acceleration of 50*g* was applied to the experimental cases shown in Table 1. Static horizontal loading tests were conducted such as to achieve a horizontal displacement of the piles at the ground surface of 1 % or greater than the pile diameter without residual displacement in the pile or the surrounding ground. For the dynamic excitation test, one excitation was performed with the sinusoidal wave shown in the table.

Table 1. Experimental cases for PCP.

PCP (D:300mm) Case	Model ground	Ground improvement wall: Wall thickness	Ground improvement wall: Spacing from the center of the outermost pile	Ground improvement wall: Unconfined compression strendth q_u	Input seismic motion
Without	Volcanic ash soil $D_r = 85\%$ $R_{L20} = 0.242$ $[DA = 5\%]$ Layer thickness 300 mm (15.0 m)	-	-	-	20 sine waves Frequency (1.5 Hz) Max. Acc. (200 cm/s^2) Single excitation
4D-1000		20mm (1.0m)	24mm (1.2m)	902kN/m^2 [Age 11 days]	
6D-1000			36mm (1.8m)	861kN/m^2 [Age 11 days]	

* Case names represent the spacing from piles and target strength of ground improvement wall.
* "Without" is "without the improvement wall." * D: Pile diameter. ( ): Prototype scale.

For the model PCP, an aluminum pipe with a diameter D = 6 mm and wall thickness t = 0.5 mm was used. This corresponds to a prototype scale equivalent of D = 300 mm and a bending stiffness EI = 1.408 × 10^4 kN·m^2. PCPs constructed before the introduction of current seismic standards often used D = 300 mm and EI = 9.940 × 10^3 kN·m^2. This study represented them by approximating those EI values.

The model piles were arranged as a set of four piles (2 × 2) with a pile center-to-center $3D$ (D = pile diameter) for each pile type. Strain gauges were attached to one of the four piles at 11 depths (two gauges per depth). The mass of the pile head weight differed from that in the SPP and CCP experiments. This was because the vertical pile head load per unit cross-sectional area of the model pile was set to be equivalent to the average vertical pile head load of existing small to medium-sized bridges (1,249 kN/m² at prototype scale).

The separation was set to $4D$ and $6D$ from the center of the outermost pile, ensuring that there would be no contact with the existing footing. The improvement strength of the wall was set with a target uniaxial compressive strength q_u of 1,000 kN/m².

Due to experimental process constraints, early-strength Portland cement, which achieves the target strength at 11 days, was used as the material for the wall. The amount of soil improvement material was determined based on prior mix design tests with the model soil material. The cement was mixed with the model soil material as a slurry with a water–cement ratio (W / C) of 1.0 in a vacuum mixer. The mixed material was then poured into formwork of the specified dimensions, cured in air for 3 days, and installed in the experimental soil tank to form the model soil. The q_u values in Table 1 are those of test pieces that were prepared separately at the time of formwork placement and were cured in air until the day of the experiment. These test pieces achieved strengths close to the target values.

For the model ground, volcanic ash from the Shikotsu pumice flow deposit (Spfl), which is a characteristic volcanic ash coarse-grained soil in Hokkaido, was used. The fraction that passed a sieve with a mesh size of 0.85 mm was used to achieve a relative density D_r of 85 % and a liquefaction strength ratio R_{L20} of 0.242. This study aimed to achieve an R_{L20} of approximately 0.2 for the model soil. This value is typically attained by setting D_r to about 50 % in standard sandy soils. However, it has been noted that for volcanic ash soils, whose particle density is lower than those of sandy soils, D_r must be set to a relatively high density (85 %) (Egawa et al., 2015). Where, the liquefaction strength ratio R_{L20} is the cyclic stress amplitude ratio $\sigma_d / 2\sigma'_0$ (σ_d: cyclic deviator stress, σ'_0: effective confining pressure) that corresponds to the double amplitude axial strain DA = 5% and the number of cycles N_c = 20 in the cyclic undrained triaxial test on soils (JGS0541-2020: Japanese Geotechnical Society. 2020).

For the pore fluid in the model soil, degassed silicone oil with a viscosity of 50 cSt was used to satisfy the similarity laws for the accumulation and dissipation of excess pore water pressure. The model ground was saturated by slowly infiltrating silicone oil from the bottom of the experimental soil tank while applying negative pressure after degassing the prepared model ground.

The above experimental conditions and model fabrication conditions are identical to those of the SPP and CCP experiments, except for the model pile conditions.

3 EXPERIMENT RESULTS

In observations when the model was dismantled after the experiment, no damage was found in the ground improvement walls in any case, including wall inclination damage.

The sampling intervals for the various measurements in the centrifuge model experiments were 1.0 sec. for the static horizontal loading tests and 0.01 sec. for the dynamic excitation tests, which were derived by referencing the prototype scale. The values, including the measured ones, in the sections after this will be expressed as those for the prototype scale.

3.1 Depth distribution of measurement values related to liquefaction

Figure 3 compares the depth profiles of various measurements within the walls and in the ground without improvement measures.

The ground shear strain was derived from the acceleration time history at each depth. Specifically, the acceleration records were double-integrated to obtain the displacement time history at each measurement point. The shear strain time history was then calculated by dividing the relative displacement between adjacent depths by their vertical interval. The maximum values of these strains are plotted at the midpoints of each depth interval. The excess pore water pressure is defined as the value at 20 sec. from the start of shaking when the amplitude due to shaking has stabilized. The bending moment of the pile is obtained by averaging the positive and negative absolute values for each amplitude of the time history, and the maximum values are plotted.

Regarding the results for the PCP without countermeasures in Figure 3(a), the ground shear strain tends to increase between G.L. –3.0 m and –5.0 m, and between G.L. –8.0 m and –10.0 m, similar to the results for the SPP and CCP without countermeasures. Here, the shear strain in the

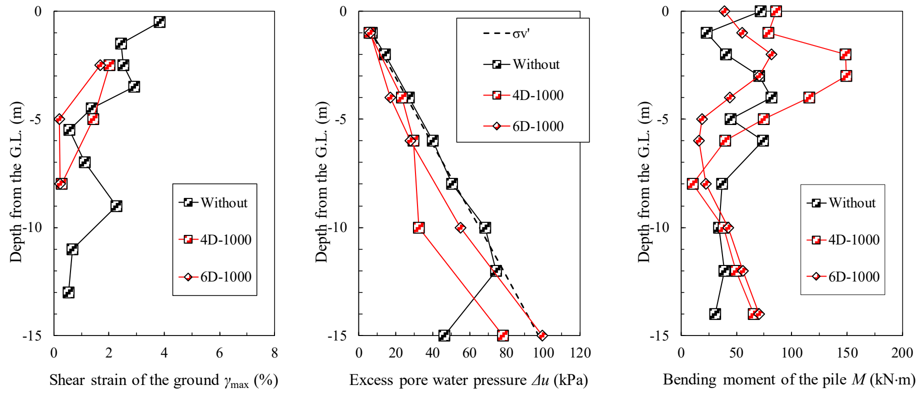

(a) PCP (equivalent to prototype scale: D = 300 mm, EI = 1.408 × 10⁴ kN/m²)

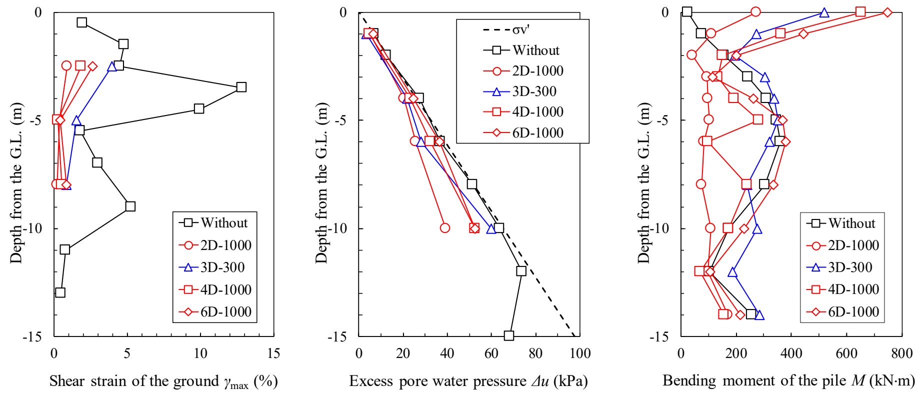

(b) SPP (equivalent to prototype scale: D = 500 mm, EI = 1.053 × 10⁵ kN·m²) (Egawa et al., 2024)

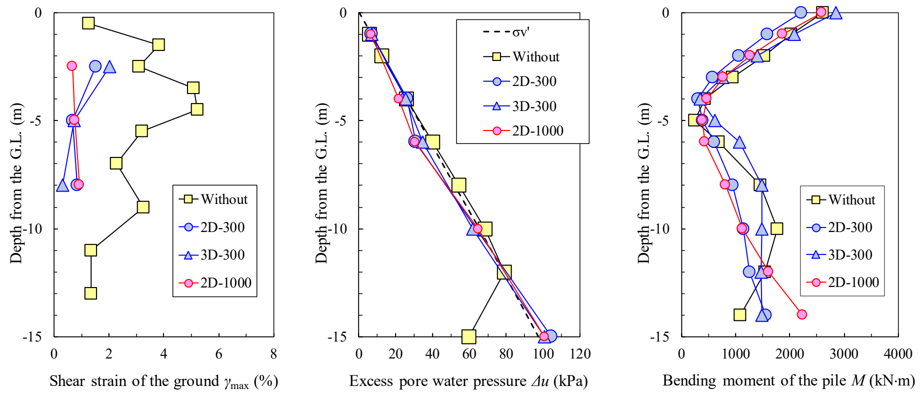

(c) CCP (equivalent to prototype scale: D = 1,000 mm, EI = 1.094 × 10⁶ kN/m²) (Egawa et al., 2024)

Figure 3. Comparison of depth distributions for maximum values of various measured parameters. (From left: shear strain, excess pore water pressure, bending moment)

untreated case for PCP tends to be smaller at depths of 3.0–5.0 m compared to the untreated cases for SPP and CCP. This may be attributed to slight local variations in soil density caused by the complex particle shapes characteristic of volcanic ash, despite aiming for the same target density in all cases. While this study focuses on the relative evaluation of mitigation effects for each countermeasure, the detailed mechanism by which these subtle initial differences affect deformation behavior remains a subject for future research. The excess pore water pressure also shows a similar trend and values to those for SPP and CCP without countermeasures. These results indicate that, when assessing the applicability of grid-form ground improvement walls to various existing pile types, it is reasonable to assume that the soil behavior inside the improvement walls is approximately equivalent to that of unimproved ground. This assumption provides consistent and acceptable results, despite differences in pile material, diameter, and stiffness. Regarding the depth distribution of pile bending moment, the values are smaller for PCP than for SPP and CCP, and the depth at which maximum values occur is shallower, except near the ground surface. This is a reasonable result, as the *EI* for PCP is smaller than

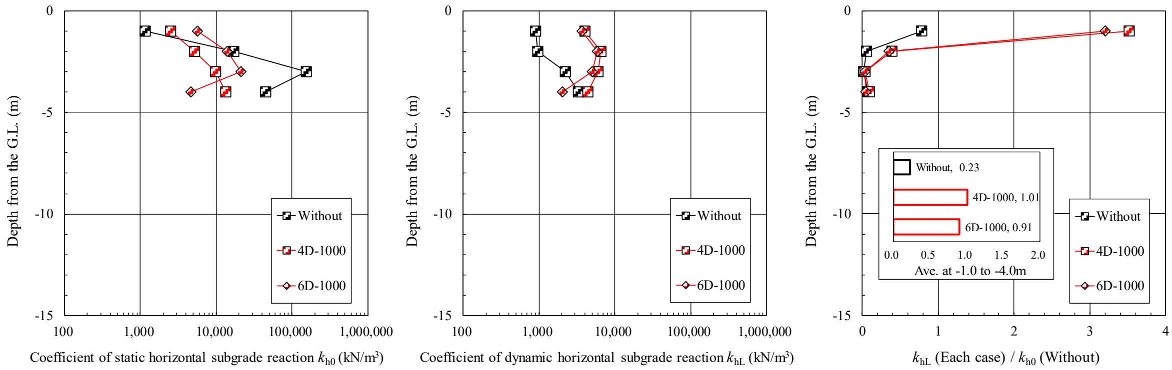

(a) PCP (equivalent to prototype scale: D = 300 mm, EI = 1.408 × 10⁴ kN/m²)

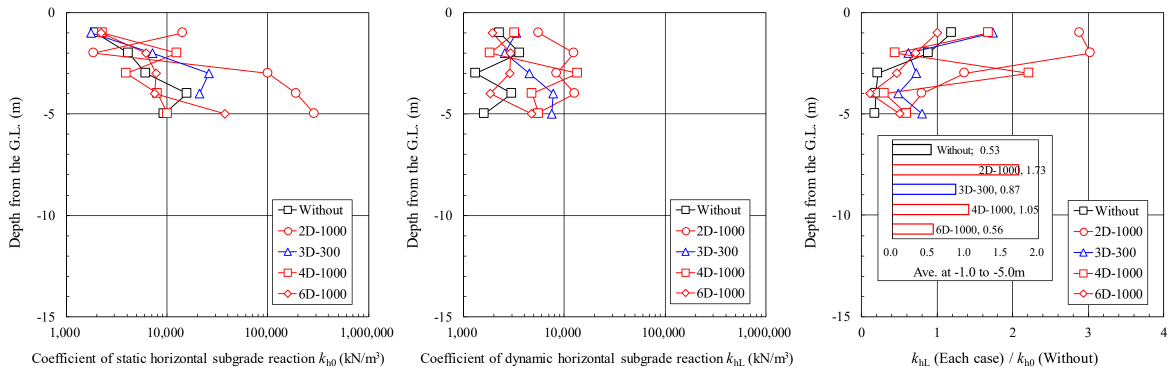

(b) SPP (equivalent to prototype scale: D = 500 mm, EI = 1.053 × 10⁵ kN·m²) (Egawa et al., 2024)

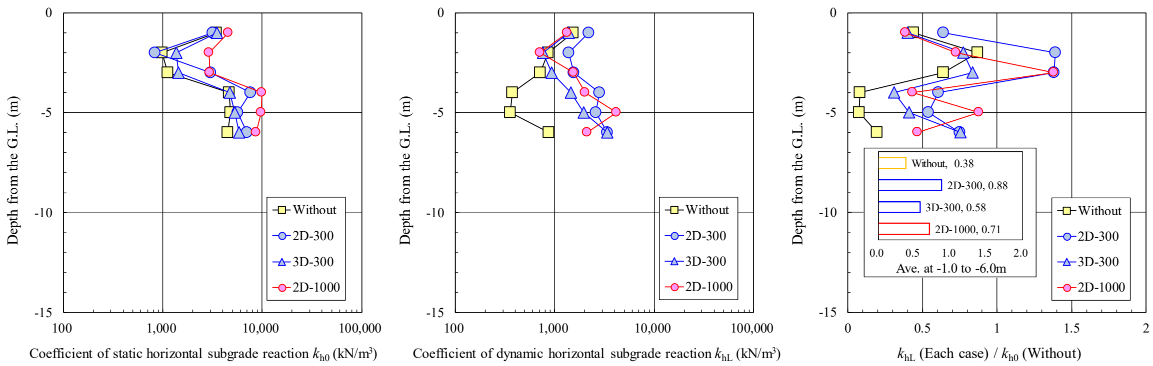

(c) CCP (equivalent to prototype scale: D = 1,000 mm, EI = 1.094 × 10⁶ kN/m²) (Egawa et al., 2024)

Figure 4. Trend of changes in pile horizontal subgrade reaction coefficient due to liquefaction.
(From left: static horizontal subgrade reaction coefficient k_{h0}, dynamic horizontal subgrade reaction coefficient k_{hL}, increase/decrease ratio k_{hL}(each case) / k_{h0}(without))

that for SPP and CCP, resulting in a shallower characteristic length of the pile (Over what depth the pile feels the soil response).

Regarding the results for the countermeasure case with PCP applied in Figure 3(a), the occurrence of ground shear strain and excess pore water pressure tends to be suppressed, compared to the case without countermeasures. Bending moment generation is suppressed at G.L. –6.0 m and G.L. –8.0 m, but at other depths, it is equivalent to that in the case without countermeasures and is greater than that in the case without countermeasures at G.L. –1.0 m to –3.0 m.

No clear trend in countermeasure effectiveness based on separation is observed in any measurement values; however, greater bending moment is generated near the pile head for PCP4*D*-1000. This is considered to be because even when the separation is set to four times the pile diameter, the separation is only 1.2 m, resulting in proximity between the walls and the existing piles, and because the dynamic horizontal ground reaction is great, which we will describe later.

3.2 Depth distributions of measured values related to seismic capacity

Figure 4 shows the increase/decrease in the horizontal soil reaction coefficient k_{hL} / k_{h0} for piles associated with liquefaction in volcanic ash ground. k_{hL} / k_{h0} is the ratio of the dynamic horizontal soil reaction coefficient k_{hL} during vibration to the static horizontal soil reaction coefficient k_{h0} for each case without countermeasures applied before vibration. Note that the values for k_{h0} and k_{hL} are those at a pile surface displacement of 1 % of the pile diameter. The procedures for calculating each are detailed in Egawa et al. (2018). Here, we compared the values of k_{hL} / k_{h0} at depths where the static horizontal soil reaction coefficient of the pile prior to vibration was clearly obtained in all cases. (PCP: G.L. –1.0 m to –4.0 m, SPP: G.L. –1.0 m to –5.0 m, CCP: G.L. –1.0 m to –6.0 m).

Regarding the k_{h0} values for PCP, SPP, and CCP under the no-countermeasure case in Figure 4(a), the values tend to be greater for PCP than for SPP or CCP. This aligns with the general finding that, under identical ground conditions, smaller pile diameters result in greater horizontal ground reaction forces per unit area.

From Figure 4(a), both PCP4*D*-1000 and PCP6*D*-1000 exhibit k_{h0} values comparable to or smaller than those for the no-countermeasure cases. Considering the experimental results for the other pile types, it is considered that maintaining a separation of at least 4*D* prevents excessive increases in k_{h0}. The k_{hL} values of PCP4*D*-1000 and PCP6*D*-1000 during vibration testing tended to be greater near the ground surface than for pre-vibration levels and tended to decrease with increasing depth. However, no clear differences were observed to occur with differences in separation.

The horizontal subgrade reaction coefficient used in the design of road bridge pile foundations is specified to be the average value up to a depth of the pile's characteristic length, which represents the pile's horizontal resistance zone. Furthermore, for soil layers judged to be susceptible to liquefaction, soil parameters such as the horizontal subgrade reaction coefficient (including the subgrade reaction coefficient, upper limit of subgrade reaction force, and maximum shaft friction) are reduced by multiplying them by a reduction factor D_E, and seismic performance verification is conducted. In this study, the increase/decrease ratio k_{hL} / k_{h0} was used as an indicator corresponding to D_E to confirm the effects of the walls and pile and the improvement strength on the pile foundation. The figure also shows the average values of k_{hL} / k_{h0} at the depths where they are plotted.

The SPP results in Figure 4(b) show that in the case with a separation of 2*D* (1.0 m), the average value of k_{hL} / k_{h0} exceeds 1.0, indicating a greater dynamic horizontal subgrade reaction force than that before vibration in the case without countermeasures. This suggests that measures that require structural improvements to the entire bridge system are necessary.

The CCP results (Figure 4(c)) show that in the case with separation 2*D* (2.0 m), k_{hL} / k_{h0} exceeded 1.0 at certain depths, but the average value was lower than that before vibration in the case without countermeasures. Therefore, it was considered that measures that require structural improvements to the entire bridge system were *not* necessary for these cases.

The PCP results (Figure 4(a)) show that since no clear difference in the depth distribution of k_{h0} and k_{hL} was observed between the two separations, the k_{hL} / k_{h0} values also showed similar trends for PCP4*D*-1000 and PCP6*D*-1000. The average k_{hL} / k_{h0} values for PCP4*D*-1000 and PCP6*D*-1000 were generally around 1.0. This is roughly equivalent to the horizontal subgrade reaction of the piles without countermeasures before vibration, indicating that the reduction in the horizontal subgrade reaction coefficient of the piles due to liquefaction is being suppressed. However, examining values by depth reveals that dynamic horizontal subgrade reaction forces act significantly near the ground surface, decreasing to values indistinguishable from those without countermeasures at G.L. –3.0 m to –4.0 m. This suggests that even when the separation is set to four times or six times the pile diameter (1.2 m or 1.8 m), the distance remains relatively short. Consequently, piles near the ground surface, where pile head displacement is large, are likely to experience significant horizontal subgrade reaction forces from the ground improvement wall. When this method is applied to small-diameter piles, it is necessary to implement measures that account for the high horizontal soil reaction near the ground surface and its significant variation along the depth. Furthermore, experimental results for small-diameter PCPs suggest that the separation distance at which the walls influence existing piles depends on the absolute distance rather than on a value derived by multiplying the pile diameter.

4 DISCUSSION ON HOW LIQUEFACTION CONTROL EFFECTIVENESS DIFFERS WITH DIFFERENCES IN SEPARATION AND GROUND IMPROVEMENT STRENGTH

This section examines the effectiveness of grid-form ground improvement wall techniques in suppressing excess pore water pressure and examines the influence of those techniques on the horizontal subgrade reaction coefficient of piles.

Figure 5(a) shows the relationship between the grid spacing and the excess pore water pressure ratio inside the walls. The grid spacing L was divided by the improvement depth H to give a generalized dimension ratio L / H. The excess pore water pressure ratio Δu / σ_v' is the excess pore water pressure Δu divided by the effective overburden pressure σ_v'. The Δu / σ_v' values for each experiment case were calculated at each measured depth of excess pore water pressure in Figure 4 and represent the average value between G.L. –1.0 m and –10.0 m.

Figure 5(a) shows that the smaller is the separation, the greater is the suppression of Δu / σ_v'. Furthermore, focusing on the values for separation $4D$ in SPP and separation $2D$ in CCP, it is evident that the greater is the improved strength, the greater is the suppression of Δu / σ_v'.

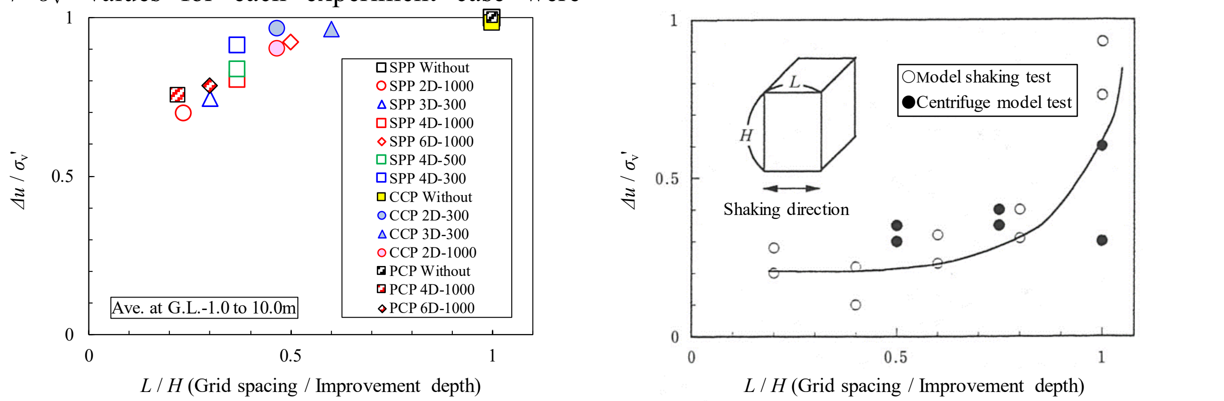

(a) Volcanic ash ground *(b) Sandy ground (Ministry of Construction, PWRI., 1999)*

Figure 5. Relationship between dimension ratio L/H and Δu / σ_v' inside the ground improvement walls.

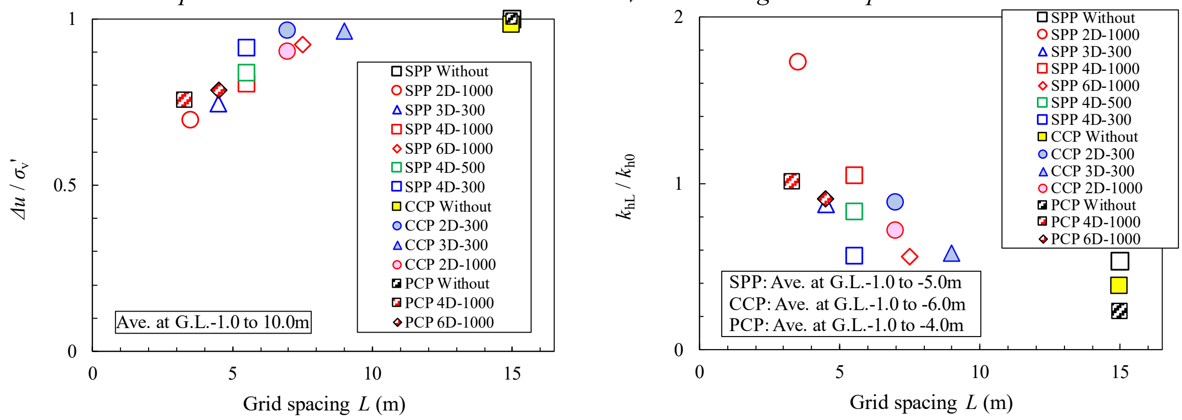

(a) Δu / σ_v' *(b) k_{hL} / k_{h0}*

Figure 6. Relationship between grid spacing L and Δu / σ_v', k_{hL} / k_{h0} in volcanic ash ground.

For comparison, Figure 5(b) shows the results published in the Cooperative Research Report by the Public Works Research Institute (1999), in which a study similar to the current one was conducted on sandy ground. This indicates that for sandy ground, there is also a correlation between the dimensional ratio and the effectiveness of suppressing excess pore water pressure. However, it is understood from the figures that the extent of this difference differs between volcanic ash ground (a) and sandy ground (b). This study indicates that previous studies and standards for sandy ground cannot be applied directly to volcanic ash ground. Therefore, it is necessary to develop design techniques adapted to the liquefaction behavior of volcanic ash ground and for the pile foundation behavior in such ground.

The liquefaction layer thickness in this current examination (a) is 15.0 m. The liquefaction layer thicknesses in a previous study on sandy ground (b) are 0.4 m in the model vibration test and 10.0 m in the centrifuge model test, and the area and volume enclosed by the walls in (a) and (b) are different.

Figure 6(a) shows L / H in Figure 5(a) as L. Figure 6(b) shows the relationship between L and k_{hL} / k_{h0}.

This study on sandy ground indicates that, based on the relationship shown in Figure 5(b), the improvement walls are effective in suppressing Δu / σ_v' inside the walls in the range where L / H is smaller than about 0.8. Applying $L / H = 0.8$ to the centrifuge model experiment shown in Figure 5(b), L corresponds to 8.0 m. Although the degree of effectiveness in volcanic ground differs from that in sandy ground, volcanic ash ground also shows suppression of Δu / σ_v' within the walls in the range where L is less than approximately 8.0 m, regardless of pile type, as seen in Figure 6(a). Figure 6(b) shows that k_{hL} / k_{h0} tends to be great when L is smaller than about 7.0 m and that when L is less than about 4.0 m, the horizontal subgrade reaction coefficient exceeds 1.0 and is higher than that of the case without countermeasures.

Furthermore, based on experimental results for PCPs with small diameters, the separation at which the improvement walls affect existing piles appears to depend on the actual distance of separation rather than on the numbers derived by multiplying the pile diameter. Therefore, L, from Figure 6(b), was shown in Figure 7 as the actual distance from the center of the outermost pile. The results show that k_{hL} / k_{h0} does not significantly exceed 1.0 at separations greater than 2.0 m.

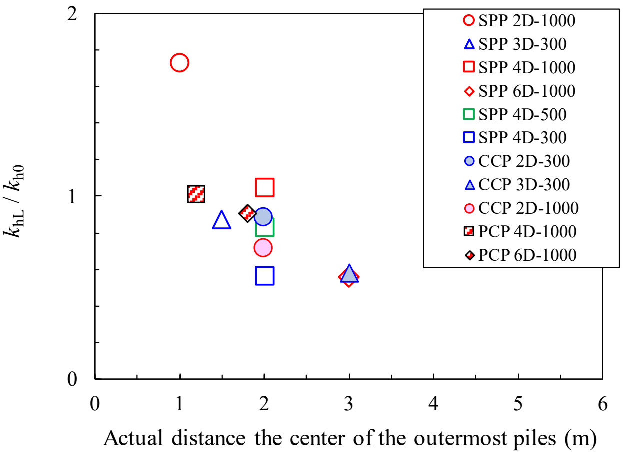

Figure 7. Relationship between actual distance and k_{hL} / k_{h0}

Furthermore, for SPP2*D*-1000, PCP4*D*-1000, and PCP6*D*-1000, which have small separation from existing piles, it was confirmed in previous chapters that a great dynamic horizontal subgrade reaction and bending moment occurs in existing piles.

Based on these findings, when this method is applied to volcanic ash ground, the grid spacing should be set to 7.0 m or less regardless of pile type. For the separation from the center of the outermost pile to the wall, a minimum of 2.0 m should be used as a guideline based on actual distance rather than on a multiple of the pile diameter. This ensures that the method does not affect the seismic design calculations for the bridge's superstructural members or the entire bridge system while achieving suppression against the reduction in the horizontal subgrade reaction coefficient of piles due to liquefaction. Within this range, the combination with the improved strength can be set according to the required performance.

5 CONCLUSIONS

This study aimed to confirm the applicability of grid-form ground improvement wall techniques for the seismic reinforcement of road bridge pile foundations in volcanic ash ground, considering liquefaction effects. The focus was on verifying suitability for SPP, CCP, and PCP piles with varying diameters and stiffnesses. Findings were derived from centrifugal model tests that varied the distance of the outermost pile center from the wall and the improvement strength. Based on these findings, when these techniques were applied to volcanic ash ground, it was clarified that the grid spacing should be set to 7.0 m or less regardless of the pile type. For the separation distance of the wall from the center of the outermost pile, a minimum of 2.0 m should be used as a guideline based on actual distance rather than on separation based on the pile diameter. This ensures that the method does not affect the seismic design calculations for the bridge's superstructural members or the entire bridge system while achieving suppression against the reduction in horizontal subgrade reaction coefficient of piles due to liquefaction. Within this range, the combination of these setting with improved strength adjustment can be set according to the required performance.

REFERENCES

Egawa, T., Yamanashi, T. and Tomisawa, K. (2015). Study on horizontal subgrade reaction of piles in volcanic ash ground during liquefaction. *Proceedings of the 6th ICEGE 2015*, Paper No. 155.

Egawa, T., Yamanashi, T. and Isobe, K. (2018). Investigation on the aseismic performance of pile foundations in volcanic ash ground. *Proceedings of the 9th ICPMG 2018*, pp. 879-884. https://doi.org/10.1201/9780429438646-17

Egawa, T., Hayashi, H. and Isobe, K. (2024). Centrifuge model tests on liquefaction countermeasure for road bridge pile foundations in volcanic ash ground. *Proceedings of the 5th ECPMG 2024*. ECPMG2024-26. https://doi.org/10.53243/ECPMG2024-26

Ministry of Construction, Public Works Research Institute, Seismic Technology Research Center, Soil Dynamics Laboratory, et al. (1999). Manual for Liquefaction Countermeasure Construction and Design (Draft). *Joint Research Report of the PWRI*, No. 186 (in Japanese).